PROCEEDINGS, 48th Workshop on Geothermal Reservoir Engineering
Stanford University, Stanford, California, February 6-8, 2023
SGP-TR-224

Modeling and Analysis of Stimulation and Fluid Flow in the Utah FORGE Reservoir

Sang H. Lee and Ahmad Ghassemi

Reservoir Geomechanics and Seismicity Research Group, The University of Oklahoma, Norman, OK, USA

ahmad.ghassemi@ou.edu

Keywords: Geothermal, Reservoir Simulation, Discrete Fracture Network, Utah FORGE, EGS, Reservoir Stimulation, Seismicity

ABSTRACT

In this paper we simulate fluid flow and energy transport in the stimulated rock mass at the toe of the injection well in the Utah FORGE. First, we verify the numerical approach with an analytical model for heat transport in a single fracture in hot impermeable rock. After that, using reservoir data during stimulation, we estimate the rock mass permeability and investigate the fluid flow capacity from the injection well to the production wellbore through the fracture network resulting from the Stage3 hydraulic stimulation of the Well16(A)78-32. The influence of fracture geometry and stimulated permeability change on fluid flow in response to step-rate injection schedule is also assessed. Both the numerical calibration of the permeability using the pressure and pumping rate and the seismic events triggering fronts analysis show good approximation in FORGE reservoir permeability. The study helps assess the best location for the planned production well and is useful for measurements aimed at characterization of the rock mass transport properties.

1. INTRODUCTION

In this work, we present numerical modeling of fluid flow by focusing on the hydraulic stimulated zones at the toe of Well 16A(78)-32 in Utah FORGE. The FORGE (Frontier Observatory for Research in Geothermal Energy) site is located 250 km south of Salt Lake City, Utah. The field experiment aims to help improve drilling, stimulation, and circulation technologies for Enhanced Geothermal Systems development. The injection Well 16A(78)-32 is highly deviated, up to 65 degrees, and the temperature at the target zone is around 225 degrees Celsius. The intact rock permeability is very low (Zhou and Ghassemi) but many cracks and fractures in the reservoir enhance the fluid flow and heat exchange capacity for the extraction of geothermal energy. More than 2000 natural fractures have been identified, however, DFIT test results indicate that the rock permeability is still not enough to allow water to circulate between the wells (Moore et al., 2019, Xing et al., 2021, Xing et al., 2022). To improve the fluid flow, well stimulation by hydraulic fracturing has been planned and carried out to enhance fluid circulation potential of the planned doublet.

Modeling of the Utah fracture reservoir rock mass can be done using a discrete fracture network approach (Ratnayake and Ghassemi, 2022) with the fractures explicitly considered. In our work, we consider the equivalent permeability of the discrete fracture network around the stimulated zone. The fluid flow and heat transport are simulated using a finite-difference method with stress-dependent permeability. First, the model is verified using a theoretical model for heat extraction by circulating water in a fracture in geothermal reservoir (Cheng and Ghassemi, 2001, Lowell 1976), then the simulation model is compared with a lab-scale EGS experiment to observe the impact of induced fracture on the heat mining by fluid circulation in a mini-EGS reservoir (Hu and Ghassemi, 2020). After the numerical model verification, the field-scale numerical simulations are carried out to analyze the circulation potential and the expected pressure and temperature variations in the Utah FORGE stimulated reservoir volume (SRV). The model has been calibrated based on the FORGE pressure observations during the stimulation process and used to estimate the stimulated volume around the Well 16A(78)-32 and its permeability. In addition. the induced microseismic clouds for 3-stage hydraulic stimulations are also analyzed to obtain the permeability based on the concept (Shapiro et al., 1997) of the triggering front in an effective isotropic homogeneous poroelastic rock. The results of both approaches are compared in relation to the stimulation outcome and flow potential with reference to the concept of flow impedance.

2. NUMERICAL MODELING

Fluid flow, and heat transport in EGS has been extensively studied in the past decades using the boundary and finite element methods (Cheng et al., 2001; Ghassemi et al., 2003, 2005, 2007, 2008; Zhou et al., 2009; Ghassemi and Zhou, 2011; Rawal and Ghassemi, 2014; Safari and Ghassemi, 2015 and 2016; Xia et al., 2017; Gao, Q., Ghassemi, A. 2020). In this work, we utilized a finite difference method (Kipp, et al., 2008) and consider a stress dependent DFN permeability model to simulate hydraulic fracturing. The model considers the conservation equations for mass, momentum, and energy balance.

2.1 Model Verification

For the coupled fracture/reservoir model, we first verify the equivalent permeability approach to represent the fracture grid-blocks in the finite-difference domain. The analytical model for temperature change by cold water injection into the fractured hot dry rock was performed by Gringarten et al. (1976), Lowell (1976), Cheng et al., (2001). Here we focused on a single fracture connecting the injector and producer to compare the temperature change by fluid flow. The model's grid-block size is 10 m for x, y, z-direction and the total number of grid-blocks used are 30, 31 and 32 in each direction. The single fracture is 300 m in length, 100 m in height, and is represented by a10 m wide zone of grid blocks as described in Fig. 1(a). For the fracture flow in finite-difference grid-blocks domain, the equivalent permeability is calculated and applied using the relationship between the Cubic's law and the Darcy's law comparing the slit flow amount within the fracture and the corresponding equivalent grid-block Darcy's flow rate. For instance, the analytical study of fracture flow in

hot geothermal rock by Cheng et at. (2001), we can derive the equivalent permeability for the following fracture L = 300 m, b = 0.03 cm, and v = 0.5 cm/s as to be k = (w3/12)/(width of grid-block) = 2.25×10-10 m2. Input parameters for the analytical model and numerical simulations are presented in Table 1. Comparison of numerical modeling and the analytical solution data for temperature change by cold water injection is presented in Figure 1(b). The simulation results show good agreement with the analytical solution except for when a cold waterfront moves into the hot rock at the relatively early stage. The numerical results of pressure and the temperature change after 15-years of fluid circulation are presented in Figure 2 and Figure 3.

Table 1: Input parameters for an analytical fracture flow model and numerical simulations

Parameter	Value
Fracture length, L	300 m
Fracture width, b	0.3 cm
Fluid velocity, v	0.5 cm/s
Heat Conductivity of rock, K_r	6.2×10^{-3} cal/cm-sec-°C
Heat capacity of rock, C_r	0.25 cal/g-°C
Heat capacity of rock, C_w	1.0 cal/g-°C
Density of rock, ρ_s	2.65 g/cm^3
Density of water, ρ_w	1.0 g/cm^3
Reservoir temperature, T_{res}	300 °C
Reservoir temperature, T_{inj}	40 °C

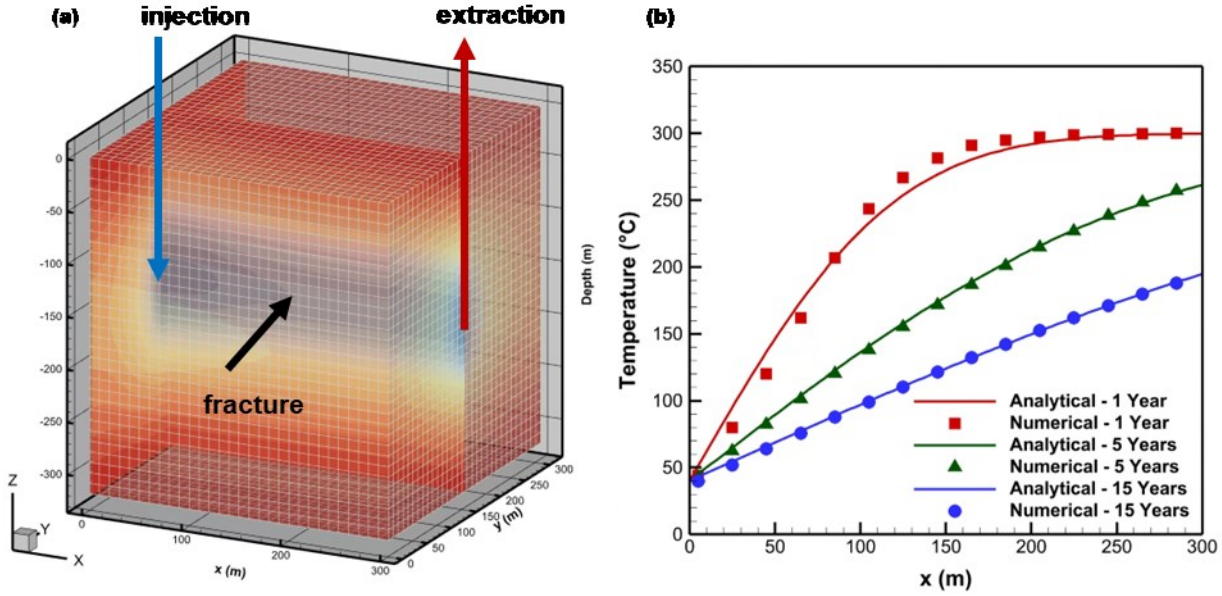

Figure 1: (a) Discretized grid model for single fracture flow between the injector and the producer. (b) Comparison of the temperature changes from the numerical simulation with the analytical solutions.

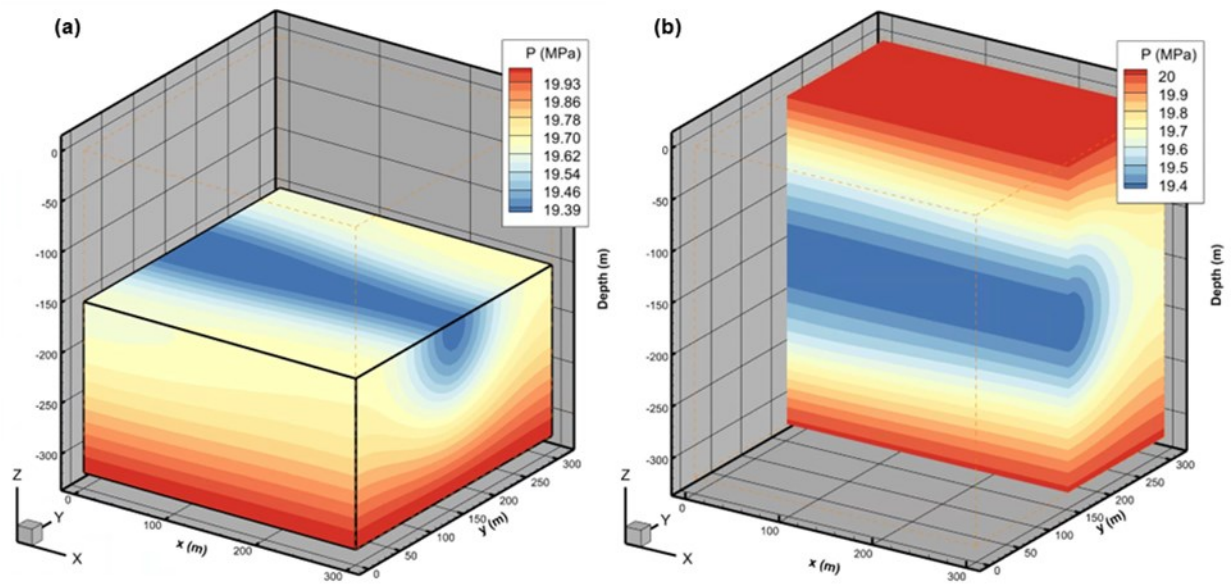

Figure 2: Nermerical model results of pressure distribution around the fracture for 15 year fluid circulation. (a) horizontal cross-section view of pressure change, (b) vertical cross-section view of pressure change.Nermerical model results of pressure distribution around the fracture for 15 year fluid circulation. (a) horizontal cross-section view of pressure change, (b) vertical cross-section view of pressure change.

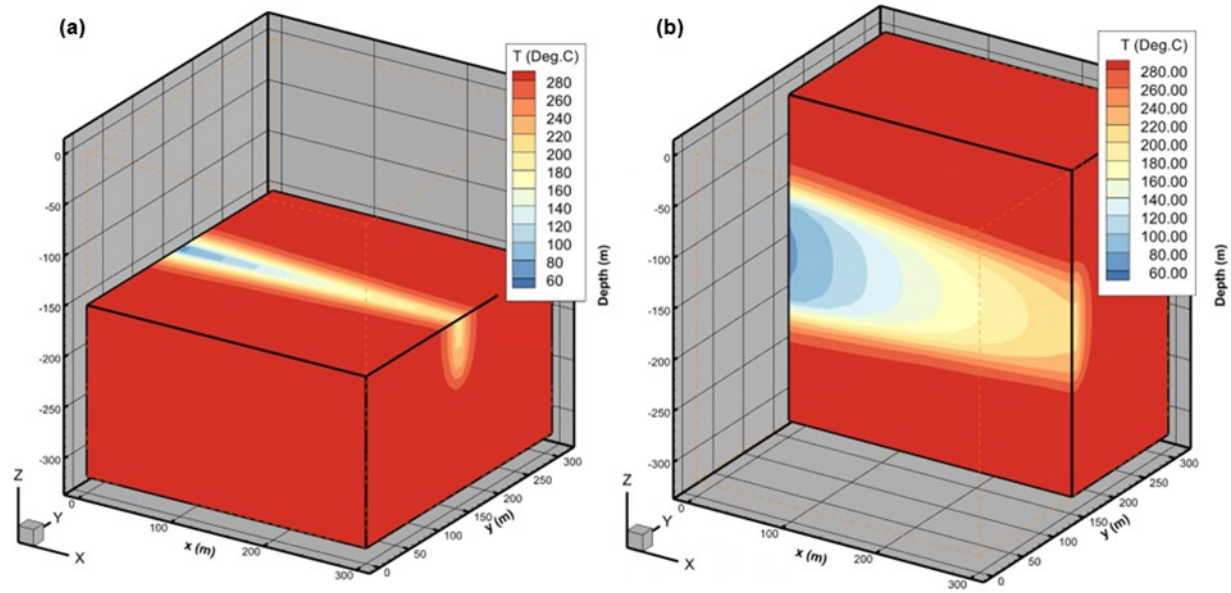

Figure 3: Nermerical model results of temperature distribution around the fracture for 15 year fluid circulation. (a) horizontal cross-section view of temperature change, (b) vertical cross-section view of temperature change.Nermerical model results of temperature distribution around the fracture for 15 year fluid circulation. (a) horizontal cross-section view of temperature change, (b) vertical cross-section view of temperature change.

2.2 Numerical Modeling of Fluid Flow in the Stimulated Rock Around Utah FORGE Well 16A(78)-32

In this section, we model a 3-stage hydraulic stimulation of Well 16A(78)-32. The coordinate of the modeling domain is UTM(m) – 333,358(m) for x-coordinate and UTM(m) – 4,261,781(m) for y-coordinate. The x- and y-coordinates are rotated 30° to align the simulation domain with the maximum horizontal stress direction (the orientation of the maximum horizontal stress is given as N30°E in Moore et al., 2019) for the meshing and computation of equivalent permeability – hydraulic fracture propagation direction. Figure 4(a) illustrates the reservoir simulation domain. The natural fractures geometry has been obtained from the FORGE Geothermal Data Repository. Figure 4(b) shows the equivalent permeability due to the discrete fracture network (DFN) distribution around the well and the location of each stage for hydraulic stimulation. The total number of grid-blocks are 65, 60, and 60, respectively, and the grid-block size for finite difference method simulation is 10m, 10m, and 10 m for x-, y-, and z-direction. The input parameters used for FORGE stimulation modeling are listed in Table 2, and the initial pressure and temperature distributions are provided by Native Stage FALCON input data from Idaho National Laboratory.

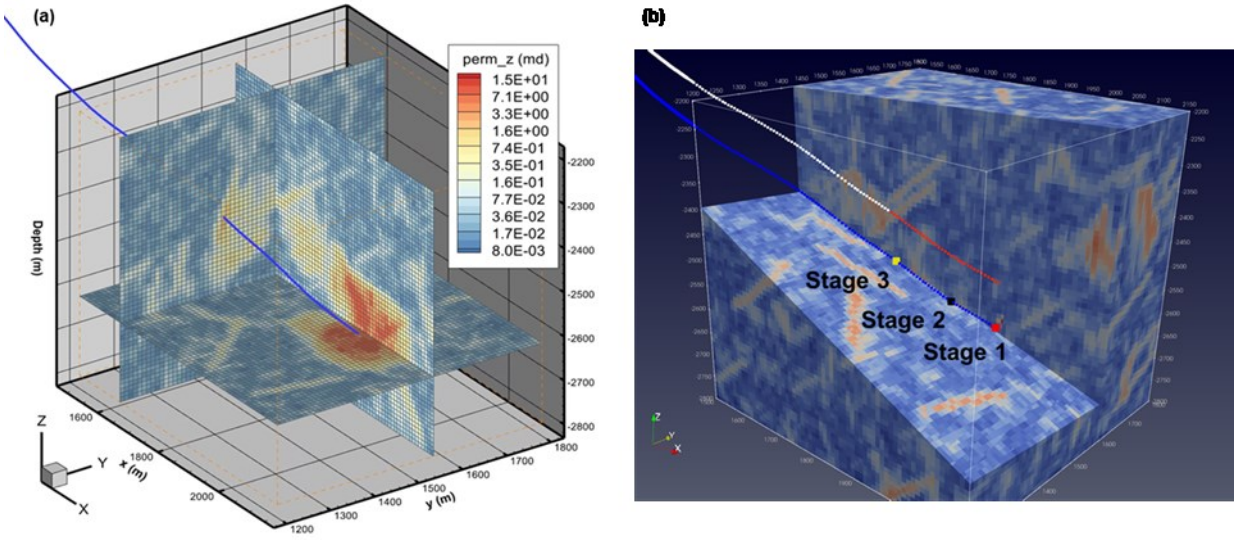

Figure 4: (a) Reservoir domain size and grid-blocks for fluid stimulation modeling of stage 1, 2, and 3. The blue line indicates the trajectory of Well 16(A)78-32. (b) DFN permeability distribution around Well 16(A)78-32. The locations of the stages are marked on the blue line as stage 1 - red, Stage 2 – black dot, stage 3 – yellow dot. The white and red line show the prospective doublet for circulation test.

Table 2: Input parameters for Utah FORGE stimulation modeling

Parameter	**Value**
Porosity, $\emptyset$	1 %
Thermal conductivity, K_T	4.0 W/m-K
Matrix permeability, K	Discrete Fracture Network upscaled permeability distribution
Heat Capacity, c_T	1200 J/Kg-K
Density of rock, ρ_s	2.7 g/cm^3
Residual saturation of water, S_{wr}	0.30
Residual saturation of steam, S_{gr}	0.05

The discrete fracture network data around those zones are used (https://gdr.openei.org/submissions/1317) to generate equivalent permeability for finite difference grid-block's property. After implementation of DFN permeability, the Gaussian smoothing process is utilized to improve the numerical stability (Figure 4(b)). For the initial permeability distribution in the numerical modeling, upscaled simplified DFN permeability data is used and processed with a Gaussian smoothing algorithm with smoothing parameter, $\sigma = 0.5$. The boundary conditions at the bottomhole is set to 31°C based on modeling using Ramey (1962) method. For instance, the inlet water temperature at the surface is assumed to be 15°C, the reservoir rock temperature gradient is 84.6 °C/km (assuming constant temperature gradient), and the flow rate is 50 Kg/sec.

To model the fluid-induced permeability increase, a pressure-dependent permeability is assumed. In particular, the permeability is assumed to increase exponentially according to the exponential relationship (Morrow and Lockner, 1994, Nathenson, 1999):

$$k = k_0 e^{\alpha(\Delta P)} \tag{12}$$

where k, k_0, α, p, p_0 are permeability, initial permeability, material constant, pressure, and initial pressure, respectively. The material parameter α is a control parameter to estimate fluid-induced permeability increase and this may adjust depending on the fracture volume and geometry. In this example study, we set α to 0.025~0.030/kPa.

Stage 3 pressure numerical modeling work is compared with field observations. In contrast with Stage 1 and Stage 2 hydraulic stimulations, the microseismic events for Stage 3 shows anisotropic clouds which suggest the localized rock failures by fluid stimulation rather than the isotropic diffusion behavior in Stage 1 and 2. Figure 5 illustrates pressure modeling compared with field data for Stage 3 hydraulic stimulation test. The bottom hole pressure is obtained by adding the hydrostatic pressure gradient (0.433 psi/ft) at 8530 ft to the wellhead pressure. The loss of pressure by longitudinal wellbore friction and near wellbore pressure drop by tortuosity and/or perforation friction are not considered in this modeling work. However, the field data is adjusted by subtracting the possible tortuosity and/or perforation friction. The estimation of pressure drops due to tortuosity is not included, but we assumed approximately 5-10 MPa pressure losses in the simulations.

The anisotropic permeability model has been applied for numerical modeling since the anisotropic microseismic events cloud observations for Stage 3. The calibrated maximum permeability is 60 md for y-direction, 30 md for z-direction, and 6 md for x-direction. After the maximum injection rate pumping, the permeability also decreased to 20 md for y-direction, 10 md for z-direction, and 2 md for x-direction. This localized permeability distribution shows good agreement with the field data and the possible localized rock failure. Note that the numerical domain is rotated 30° from the North to East direction to align with the maximum horizontal stress direction, so the anisotropic equivalent permeability could represent the average fluid path around the Stage 3 hydraulic stimulation.

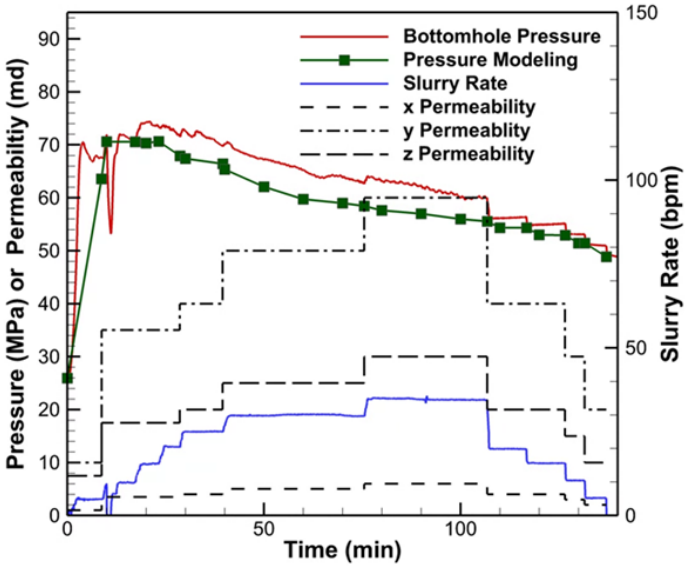

Figure 5: Pressure modeling results for Stage 3 are plotted in green line. The field pressure and injection rate are also plotted for the comparison (red - bottomhole pressure, blue – injection rate). The black line is the maximum permeability in the modeling with respect to the pumping rate. The recorded time has been shifted by t_0 = 109.6 min in the plot since the time record began from the initial pressure testing. The anisotropic permeability model has been implemented to match the anisotropic microseismic events clouds. The highest permeability is in y-direction (the maximum horizontal stress direction), the intermediate permeability is in z-direction (the vertical stress direction), and the lowest permeability is in x-direction (the minimum horizontal stress direction).

Numerical simulations for permeability and pressure change induced by pumping rate changes for Stage 3 are presented in Figure 6 and 7. The Stage 3 permeability changes are more localized to the maximum horizontal stress direction since the model implements the anisotropic permeability model. The highest z-directional permeability and pressure distributions are presented in Figure 6(c) and Figure 7(c) each.

The iso-volume plot for pressure change from top view and side view for Stage 3 are presented in Figure 8. The volume plot is obtained by pressure change (ΔP) higher than 5 MPa, which is approximately 350 m in lateral direction and 290 m in vertical direction. Estimated stimulated volumes are also plotted around the Well 16A(78)-32 as shown in Figure 8. The stimulated volume from the numerical model is compared with the microseismic events cloud for Stage 3 in Figure 9. The SRV from the simulation with the anisotropic pressure-dependent permeability shows good agreement with the recorded seismic events.

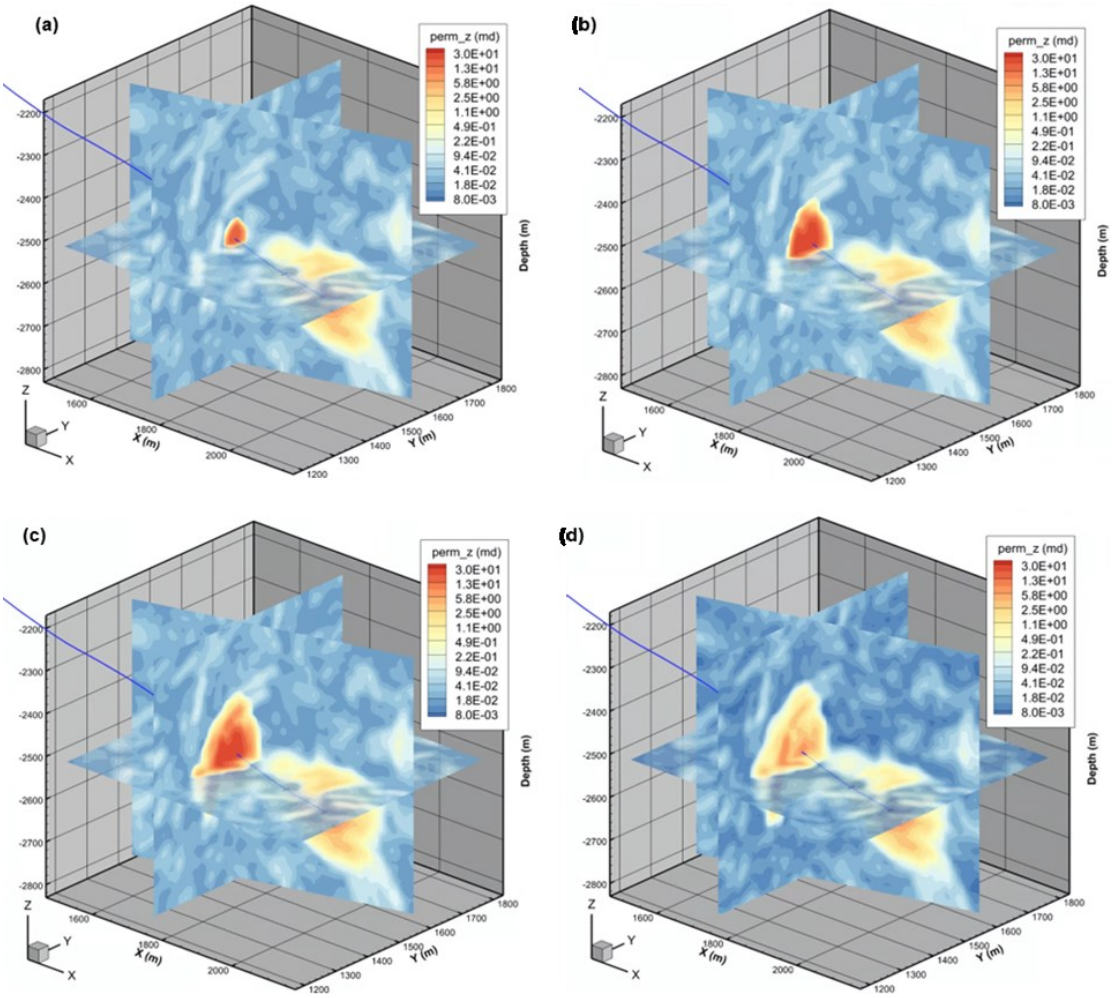

Figure 6: z-directional permeability distribution for Stage 3 at different times are plotted. (a) 20 min injection, q = 15 bpm, (b) 60 min injection, q = 30 bpm, (c) 106 min injection and the injection rate is the maximum at q = 35 bpm, (d) 137 min injection and q = 5 bpm.

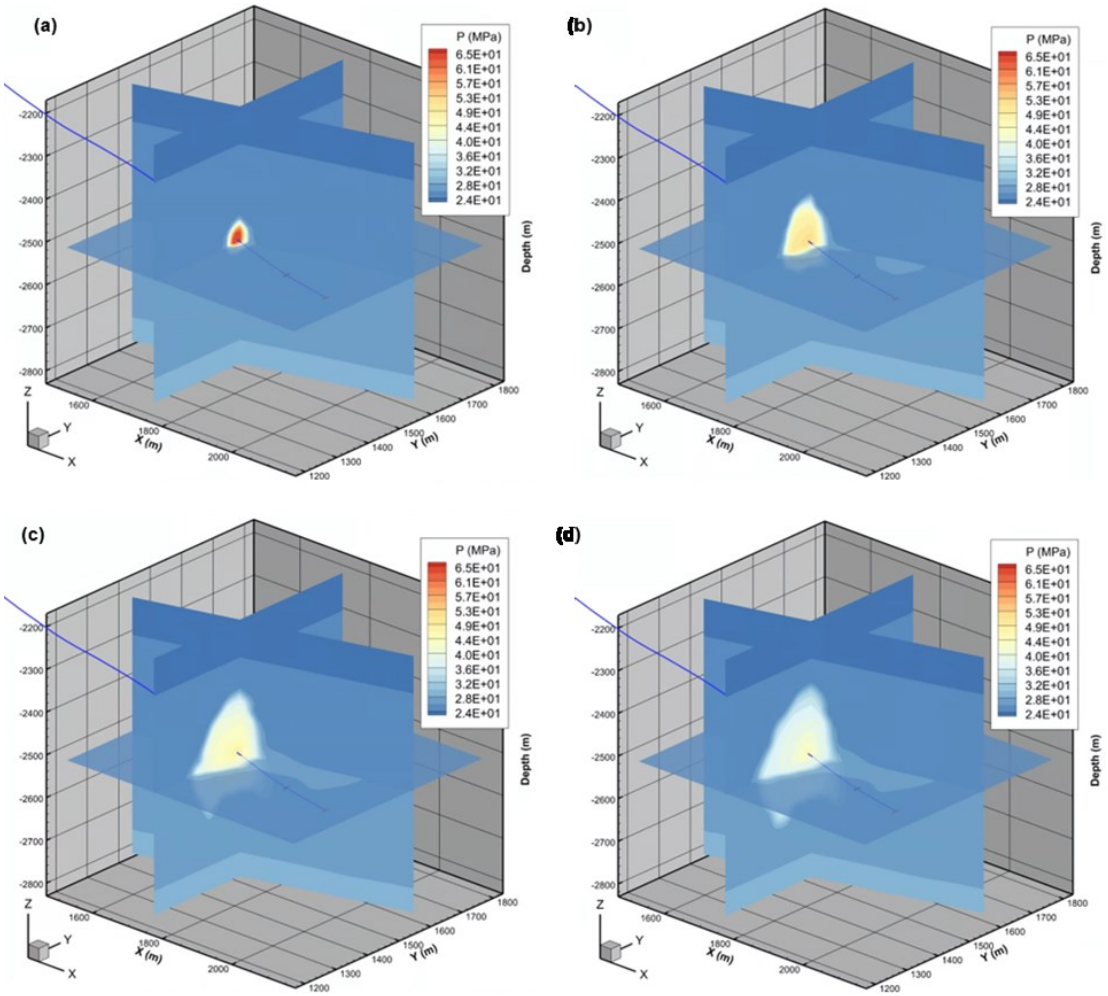

Figure 7: Pressure distribution for Stage 3 at different times are plotted. (a) 20 min injection, q = 15 bpm, (b) 60 min injection, q = 30 bpm, (c) 106 min injection and the injection rate is the maximum at q = 35 bpm, (d) 137 min injection and q = 5 bpm.

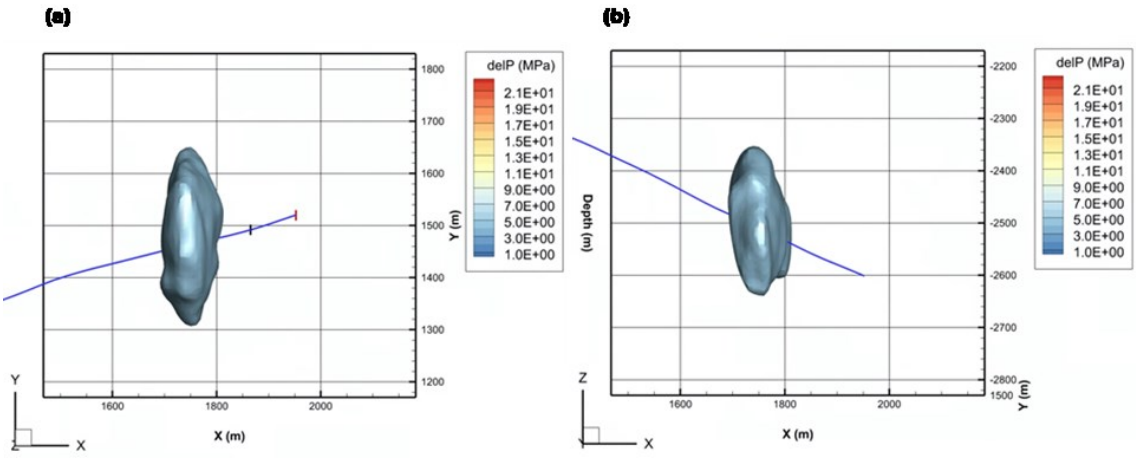

Figure 8: (a) Top view of stimulated volume after Stage 3 fluid stimulation modeling. The plot represents an iso-volume plot for delta P change higher than 5 MPa, (b) Side view of stimulated volume after Stage 3 fluid stimulation modeling. The plot represents an iso-volume for delta P change higher than 5 MPa.

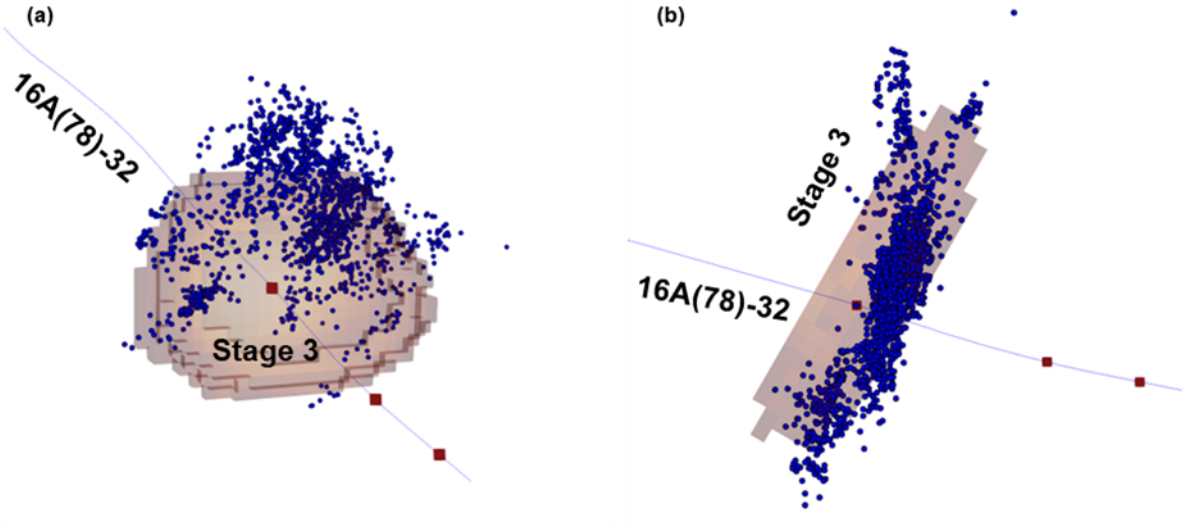

Figure 9: (a) 3D view for the comparison of modeling results of stimulated volume (light brown) and microseismic event (blue dots) for Stage 3. (b) Top view for the comparison of modeling results of stimulated volume (light brown) and microseismic events (blue dots).

3. CONCLUSIONS

A coupled fracture/reservoir model for EGS has been used to model the fluid stimulation between wells with capabilities to simulate two-phase water pressure, temperature and enthalpy change has been demonstrated. The numerical modeling was first validated with an analytical solution for a single fracture between the injector and the producer. Simulation results are in good agreement with analytical solutions for pressure and temperature change in injector and producer. Next the numerical model was carried out to analyze the Stage 3 fracturing in Utah FORGE. The results show good agreement with the pumping pressure observed in the field. Also, the stimulated reservoir volume conforms to the volume covered by the MEQ cloud recorded during stimulation. The model was used to carry out circulation between the injection and the planned production well. It was observed that an effective circulation would not be established by solely relying on the initial permeability distribution. However, with fracturing, circulation is established with an impedance value of 0.5 ~ 5 MPa/(kg/sec). This could be much more favorable if the actual natural fracture locations and geometry around the stimulation zone are more optimum. Planned field tests will provide data to address this question.

ACKNOWLEDGEMENTS

This project was supported by the Utah FORGE project sponsored by the U.S. Department of Energy, through the project "Fiber-Optic Geophysical Monitoring of Reservoir Evolution at the FORGE Milford Site."

REFERENCES

Allis, R., and Moore, J.N. "Geothermal Characteristic of the Roosevelt Hot Springs System and Adjacent FORGE EGS Site." Milford, Utah, Utah Geological Survey Miscellaneous Publication 169, Utah Department of Natural Resources, UT (2019).

Cheng, A. H.-D., Ghassemi, A., and Detournay, E. "A two-dimensional solution for heat extraction from a fracture in hot dry rock." Int. J. Numerical & Analytical Methods in Geomech., 25, 1327-1338 (2001).

Gao, Q. and Ghassemi, A. "Three-dimensional thermo-poroelastic modeling and analysis of flow, heat transport and deformation in fractured rock with applications to a lab-scale geothermal system." Rock Mechanics and Rock Engineering, 53 (2020), 1565-1586.

Ghassemi, A., and Zhou, X. "A three-dimensional thermo-poroelastic model for fracture response to injection/extraction in enhanced geothermal systems." Geothermics,40 (1), 39-49 (2011).

Ghassemi, A., Nygren, A., and Cheng, A.D.-H. "Effects of heat extraction on fracture aperture: A poro-thermoelastic analysis." Geothermics, 37 (5), 525-539 (2008).

Ghassemi, A., Tarasovs, S., and Cheng, A. H.-D. "A three-dimensional study of the effects of thermo-mechanical loads on fracture slip in enhanced geothermal reservoir." Int. J. Rock Mechanics & Min Sci., Vol. 44, pp. 1132–1148 (2007).

Ghassemi, A., Tarasovs, A. and Cheng, A.D.-H. "Integral equation solution of heat extraction induced thermal stress in enhanced geothermal reservoirs." Int. J. Num. & Anal. Methods in Geomechanics, 29, 829-844 (2005).

Ghassemi, A., Tarasovs, A. and Cheng, A.D.-H. "An Integral equation method for modeling three-dimensional heat extraction from a fracture in hot dry rock." Int. J. Num. & Anal. Methods in Geomech. 27, No. 12, 989-1004 (2003).

Ghassemi, A., Roegiers, J-C. "A three-dimensional poroelastic hydraulic fracture simulator using the displacement discontinuity method." Proceedings of the 2nd North American rock mechanics symposium, Montreal, Canada (1996).

Hu, L. and Ghassemi, A. "Laboratory Scale Investigation of Enhanced Geothermal Reservoir Stimulation." 50th U.S. Rock Mechanics/Geomechanics Symposium, Houston, TX (2016)

Hu, L. and Ghassemi, A. "Experimental Investigation of Hydraulically Induced Fracture Properties in Enhanced Geothermal Reservoir Stimulation." 42nd Workshop on Geothermal Reservoir Engineering Stanford University, Stanford, CA (2017)

Hu, L. and Ghassemi, A. "Heat and Fluid Flow Characterization of Hydraulically Induced Fracture in Lab-Scale." 52nd U.S. Rock Mechanics/Geomechanics Symposium, Seattle, WA (2018)

Hu, L., Ghassemi, A., Pritchett, J., Garg, S. "Characterization of laboratory-scale hydraulic fracturing for EGS." Geothermics, 83 (2020), 101706

Hu, L. and Ghassemi, A. "Heat production from lab-scale enhanced geothermal systems in granite and gabbro." International Journal of Rock Mechanics and Mining Sciences, 126 (2020), 104205

Kumar, D. and Ghassemi A. "A three-dimensional analysis of simultaneous and sequential fracturing of horizontal wells." Journal of Petroleum Science and Engineering, 146 (2016), 1006–1025.

Kumar, D. and Ghassemi, A. "Three-dimensional poroelastic modeling of multiple hydraulic fracture propagation from horizontal wells." International Journal of Rock Mechanics and Mining Sciences, 105 (2018), 192-209.

Lee, S. and Ghassemi, A. "Numerical Simulation of Fluid Circulation in Hydraulically Fractured Utah FORGE Well." 47th Workshop on Geothermal Reservoir Engineering Stanford University, Stanford, CA (2022)

Nathenson M. "The dependence of permeability on effective stress from fow tests at hot dry rock reservoirs at Rosemanowes (Cornwall) and Fenton Hill (New Mexico)" Geothermics, 28, 315-340, (1999)

Morrow, C.A. and Lockner, D.A. "Permeability differences between surface-derived and deep drillhole core samples" Geophysical Research Letters, 19, 2151-2154

Moore, J., McLennan J., Allis R., Pankow K., Simmons S., Podgorney R., Wannamaker P., Bartley J., Jones C., and Rickard W. "The Utah Frontier Observatory for Research in Geothermal Energy (FORGE): An International Laboratory for Enhanced Geothermal System Technology Development." 44th Workshop on Geothermal Reservoir Engineering Stanford University, Stanford, CA (2019).

Rawal, A., and Ghassemi, A. "A Reactive poro-thermoealstic analysis of cold water injection in enhanced geothermal reservoir." Geothermics, 50, 10-23 (2014).

Safari, R., Ghassemi, A. "Three-Dimensional poroelastic modeling of injection induced permeability enhancement and micro-seismicity." Int. J. Rock Mechanics. 84, 47–58 (2016).

Safari, R., Ghassemi, A. "Three-dimensional thermo-poroelastic analysis of fracture network deformation and induced micro-seismicity in enhanced geothermal systems." Geothermics, 58, 1-14 (2015).

Shapiro, S. A., Huenges, E., and Borm, G., "Large-scale in situ permeability tensor of rocks from induced microseismicity" Geophys. J. Internat., 137, 207-213 (1997).

Shapiro, S. A., Rothert, E., Rath, and Rindschwentner, J., "Characterization of fluid transport properties of reservoirs using induced microseismicity" Geophysics, 67, 212-220 (2002)

Sesetty, V.K, and Ghassemi A. "Numerical simulation of sequential and simultaneous hydraulic fracturing. Effective and Sustainable Hydraulic Fracturing", InTech (2013).

Wiles, T.D. and Curran, J.H. "A general 3D displacement discontinuity method. Proceeding of 4th Int. Conference for Numerical Methods", Geomech, (1982),103-111.

Xia, Y., Plummer, M., Mattson, E., Podgorney, R., Ghassemi, A. "Design, modeling, and evaluation of a doublet heat extraction model in enhanced geothermal systems." Renewable Energy, 105, 232-247 (2017).

Xing, P., Winkler, D., Swearingen, L., Moore, J., McLennan, J. "In-Situ Stresses and Permeability Measurements from Testing in Injection Well 16A(78)-32 at Utah FORGE Site." GRC Transactions, 45 (2021)

Xing, P., McLennan J., Moore, J. "Minimum in-situ stress measurement using temperature signatures." Geothermics, 98 (2022), 102282

Xing., P., Damjanac, B., Radakovie-Guzina, Z., A. Finnila, R. Podgorney, Moore, J., Mclenna, J. "Numerical Simulation of Hydraulic Fracturing Stimulation Enhanced Geothermal System Well at Utah Forge Site" 55th U.S. Rock Mechanics/Geomechanics Symposium, Virtual, (2021).

Zhou, X., Ghassemi, A., and Cheng, A.H.-D. “A Three-dimensional integral equation model for calculating poro- and thermoelastic stresses induced by cold water Injection into a Geothermal Reservoir.” Int. J. Num. Anal. Methods Geomech. DOI:10.1002/nag (2009).

Zhou, X., Ghassemi, A. “Experimental Determination of Poroelastic Properties of Utah FORGE Rocks.” American Rock Mechanics symposium, Santa Fe, New Mexico (2022).